ISSN 0915-633X

NATIONAL INSTITUTE FOR FUSION SCIENCE

A Note for Pitch Angle Measurement of Magnetic Field in a Toroidal Plasma Using Motional Stark Effect

J. Xu, K. Ida and J. Fujita

(Received - Mar. 13, 1995)

NIFS-349 Apr. 1995

RESEARCH REPORT
NIFS Series

NAGOYA, JAPAN

A Note on Pitch Angle Measurement of Magnetic Field in a Toroidal Plasma Using Motional Stark Effect

J. Xu, K. Ida and J. Fujita

National Institute For Fusion Science, Nagoya, 464-01, Japan

Abstract

In this letter, the spectral asymmetry of the motional Stark spectrum of a neutral beam emission in a toroidal plasma is revealed. The π component is more peaked on the more-Doppler-shifted wavelength side about the σ component, mainly owing to the existence of the angular divergence of the injected beam. A method using the σ component to measure the pitch angle in the case of a high magnetic field with an optical system containing two polarizers is also demonstrated. It is predicted that the pitch angle could be measured with an accuracy of about 2%.

keyword: motional Stark effect, pitch angle measurement

Because measurement of the pitch angle of the internal magnetic field was important for deriving the safety factor or current density profiles in a toroidal plasma, several methods that used the Faraday rotation effect[1], Laser scattering[2] and the Zeeman effect[3] were developed in the last few years. Recently, the motional Stark effect (MSE) of the Balmer α line emitted by a fast neutral hydrogen- or deuterium-beam (~50 keV/amu) in a toroidal plasma was recognized to be useful for measuring the pitch angle with high precision[4]. In DIII-D and TFTR, the pitch angle measurement that used a so-called polarimeter[4-6] was successful. For the case of a high magnetic field, an example was given by a JET experiment[7] designed with an optical system that in principle consisted of a spectrometer and two polarizers tilted with respect to the horizontal direction by $\pm 45^{o}$. The pitch angle was obtained by using the polarizers to determine the ratio of the π component intensities. Due to the overlap of each component of the MSE spectrum, especially for case of the overlap of the π emission of the full energy beam and that emitted by the half energy beam, a theoretical symmetry assumption of the Stark features is necessary to simplify retrieving of the absolute intensities, Doppler shift and wavelength splitting of each component[7,8]. The MSE spectrum is fitted by a sum of Gaussians convolved with the instrumental function of the spectrometer. Generally speaking, since there is spectral asymmetry in the spectrum as shown later in this paper, the fitting is expected to be difficult in practice due to the many parameters involved in the fitting program. In our recent research, a method utilizing the determination of the polarization direction of the σ component with the same optical system was studied, by which the pitch angle could be measured with reasonable accuracy. This letter aims to show the spectral asymmetry of the MSE spectrum and demonstrate the method using the σ lines to derive the pitch angle.

As is well known, the Balmer α line of hydrogen atom emission in an electric field is split mainly into nine components due to the Stark effect [9]. The central σ component ($\Delta m=1,-1$) is polarized perpendicular to direction of the field, while the π lines ($\Delta m=0$) distributed on both sides of the σ have parallel polarization when they are observed transversely, and are spectrally symmetric about the σ. For a beam emission in a toroidal plasma, the situation is similar due to the motional Stark effect. However, the spectral feature in this case, coupled with Doppler effect, becomes more complicated owing to the existence of angular divergence of the beam.

A simplified model may be helpful for the comprehension. In Fig.1, the beam is only a beamlet with velocity, v_b, and angular divergence, $\Delta\theta$, passing across a uniformly distributed magnetic field, B, with intersection angle, ζ, and the viewing line of the imaging system is a single line intersecting the beam with the angle, β. Supposed that there were three lines, the central σ_0 (λ_0 =6562.8 Å) and two i-th π lines at both sides of the σ_0, defined as line 1 and 2 with the wavelength being $\lambda_0-\Delta\lambda_s+\Delta\lambda_{d1}$ and $\lambda_0+\Delta\lambda_s+\Delta\lambda_{d2}$. The $\Delta\lambda_s$ is the Stark splitting here and $\Delta\lambda_{d1,2}$, the wavelength of their Doppler shift. For the case of the viewing line in the direction of the beam, one can imagine, the both angles β and ζ at point A in the figure 1 are decreased compared with the case

at position D. The Doppler shift of both the lines become increased, while their Stark splitting, $\Delta\lambda_s$, are decreased. At position E, the situation is opposite. The variation of $\Delta\lambda_s$ always tends to cancel the wavelength shift for the line 2, whereas it strengthen it for the line 1. As a result, line 2 is more peaked. The same thing will happen for line 1, if the viewing line is in direction opposite to the beam.

Quantitative differences of the wavelength width of both lines can be given as the following. Combined with the motional Stark effect, the Doppler shifted wavelength of the line 1 and 2 are given by

$$\lambda_{2,1} = \lambda_0(1 + \frac{v_b}{c}\cos\beta)(1 \pm a(i)v_b B\lambda_0 \sin\zeta), \qquad (1)$$

where, c is the light velocity and 'a(i)' is a proportional coefficient for the wavelength splitting[9]. Assuming that the emission probability of all of the original particles of the beamlet are same on the viewing line, then the wavelength width of both lines are

$$\Delta\lambda_{2,1} \cong \lambda_0(-\frac{v_b}{c}\sin\beta\Delta\beta \pm a(i)v_b B\lambda_0\cos\zeta\Delta\zeta). \qquad (2)$$

The width difference can be obtained as

$$\delta(\Delta\lambda) \cong 4a(i)v_b B\lambda_0^2\cos\zeta\Delta\theta. \qquad (3)$$

This is proportional to the beam angular divergence. Let's examine the π_3 lines of the MSE spectrum. It can be found that $2|\Delta\lambda_1-\Delta\lambda_2|/(\Delta\lambda_1+\Delta\lambda_2)$ of the π_3 lines is about 15%, if the magnetic field is 3.0 T, β is 40^o and ζ is 65^o. The $\delta(\Delta\lambda)$ may be enhanced if the variation of magnetic field in the viewed region is taken into account. The situation is similar for a beam consisting of many beamlet.

To avoid the problem mentioned above, it was found that σ component can be used to find the pitch angle in the case of a high magnetic field with the same optical system, even if the σ emission is elliptically polarized in general and is anisotropic.

Fig. 2 shows a universal situation of the σ light transmission along the viewing line. The beam and the toroidal magnetic field define a plane, the mid-plane, and the viewing line lies on it. The Lorentz electric field is in a plane perpendicular to the beam and the total magnetic field. The straight line stands for the linearly polarized part of the σ and the circle, for the circularly polarized component. The angle, α_1, is the angle of the electric field with respect to vertical direction, ψ is the angle between the electric field and the viewing line, α is the polarization angle of the σ line transmission along the viewing line and β is same as earlier definition. The relations between these angles according to the geometry are

$$\tan\alpha = \tan\alpha_1\cos\beta \qquad (4)$$

and

$$\cos\psi = \sin\alpha_1 \sin\beta. \qquad (5)$$

For the ideal case that the π manifolds are well separated from the σ components, the intensity of the σ emission is determined by each polarizer as

$$I_{1,2} = I_{\sigma c}/2 + I_{\sigma l}\cos^2(45 \pm \alpha). \qquad (6)$$

Here, $I_{\sigma c}$ and $I_{\sigma l}$ are the intensity of the circular and linear part, respectively, in the σ which are satisfied with a relation of $I_{\sigma c}/I_{\sigma l} = 2\cot^2\psi$, since the probability of the σ transition $A(\psi)=A(0)\cos^2\psi+A(\pi/2)\sin^2\psi$ (where $A(0)$ and $A(\pi/2)$ are transition probabilities when $\psi=0$ and $\pi/2$, respectively, and $A(0)=2A(\pi/2)$). The relation between the angles and the measured intensities I_1, I_2 can be obtained from equation (6) such that

$$\cot^2\psi = \frac{1}{2}\left(\frac{\xi+1}{\xi-1}\sin 2\alpha - 1\right). \qquad (7)$$

Here, $\xi = I_2/I_1$. The polarization direction of the σ component can be given as

$$\tan\alpha = \cos\beta\left\{\frac{\eta\cos\beta \pm \sqrt{\eta^2\cos^2\beta - (1+\sin^2\beta)}}{(1+\sin^2\beta)}\right\}, \qquad (8)$$

where $\eta = (\xi+1)/(\xi-1)$. The '$\pm$' operation in the equation (8) depends on η and is opposite to its sign.

As an application, the pitch angle of the internal magnetic field in the JIPP TII-U plasma was simulated using this method as depicted in Fig. 3.

Since the π components of the spectrum in the real situation may overlap with the σ component due to the broadening of the line, the validity of formula (8) was checked by our simulation. Fig. 4 shows the results. The accuracy of the pitch angle measurement can be better than 3% if the intensity of the σ lines in wavelength range of 4 Å is utilized. This result can be extended to a wide parameter range of beam and magnetic field, because the motional Stark effect of the beam emission is directly connected to the magnitude of the Lorentz electric field, as long as the Doppler shift of the wavelength of the beam emission is large enough for separation of the σ component of the full energy beam emission and the π component emitted by the half energy beam.

In practice, a filter can be used instead of the spectrometer to remove the π component because the wavelength of the σ_0 component is not effected by the magnetic field. A simulation result is also shown in Fig. 4 by the circles. It is expected that the error in the pitch angle measurement due to the mixing of the π and σ line is less than 3% if two tandemly arranged filters are used with a passband of $\Delta\lambda_p$= 2.0 Å of a Lorentz-shaped transmission curve.

In summary, the spectral asymmetry of the beam emission caused by the angular divergence of the beam in a plasma has been revealed in this letter. The π components of the spectrum are more

peaked on the more-Doppler-shifted wavelength side. To avoid problems in the method of fitting the spectrum with a spectral symmetry assumption, a method using the σ component to obtain the pitch angle information has been developed. In the case of a high magnetic field, our simulation indicates that the pitch angle can be measured with an accuracy of about 2%.

The authors would like to acknowledge Prof. M. Fujiwara for his continuous encouragement, Prof. K. Toi and Dr. A. Fujisawa for some beneficial discussion during this work. This research was supported by Grant-in-Aid for Scientific Research (B) from Ministry of Education, Science and Culture, Japan.

Reference

1. H. Soltwisch, Rev. Sci. Instrum. 59, 1939 (1988).
2. F. Alladio and M. Martone, Phys. Lett. A60, 39 (1977).
3. J. Fijita, K. McCormick, in "Proc. 8th Eru. Conf. in Controlled Fusion", 1,191 (1973).
4. F. M. Levinton, R. J. Fonck, G. M. Gammel, R. Kaita, H. W. Kugel, E. T. Powell and D. W. Roberts, Phys. Rev. Lett. 63, 2060(1989).
5. D. Wroblewski, K.H.Burrell, L.L.Lao, P.Politzer and W.P.West, Rev. Sci. Instrum. 61, 3552 (1990).
6. F. M. Levinton, Rev. Sci. Instrum. 63, 5157 (1992).
7. W Mandle, R.C. Wolf, M. Von Hellermann and H P Summers Plasma Phys. Control. Fusion 35(1993) 1373-1397.
8. R.C. Wolf, L.-G. Eriksson, M. Von Hellermann, R. Konig, W. Mandl, F.Porcelli, Nuclear Fusion, vol. 33, 1835 (1993).
9. E.U. Condon and G.H. Shortley, The Theory of Atomic Spectra (Cambridge University, Cambridge, 1963).

Figure Captions

Fig.1 Geometry schematic of an ideal diagnostic system.
A beamlet with a divergence angle $\Delta\theta$ is injected into plasma across a uniform magnetic field with an angle β. The viewing line crosses the beam with an angle ζ. Position A and E are on the viewing line where the beam has an angular divergence, $\Delta\theta$.

Fig.2 The schematic of the pattern of the σ component transmission of the beam emission along the viewing line on the mid-plane.

Fig.3 The simulated pitch angle of the internal magnetic field of the JIPP TII-U tokamak vs the major radius, with 54^{o} separation of the injected beam and the spectrum observation. The toroidal magnetic field is 3.0 Tesla, major radius, 0.93 m and the minor radius, 0.23 m in the simulation. The plasma density and temperature profile are parabolic distribution and are 5.0×10^{13} cm^{-3} and 1.0 keV at the plasma center. The input parameters of the beam are a the beam energy of 40 keV, a power ratio of each component of 0.75:0.15:0.1, an angular divergence of 0.5^{o} and a focal length of 3.0 m.

Fig.4 The expected relative error of the pitch angle measurement is calculated with the wavelength width, $\Delta\lambda$, of the σ component taken as a free parameter. The circle point curve is the expected error in the measurement for $\Delta\lambda_{p}$ =2.0 Å passband width of both filters if the transmission curvature of the filter is Lorentz shaped.

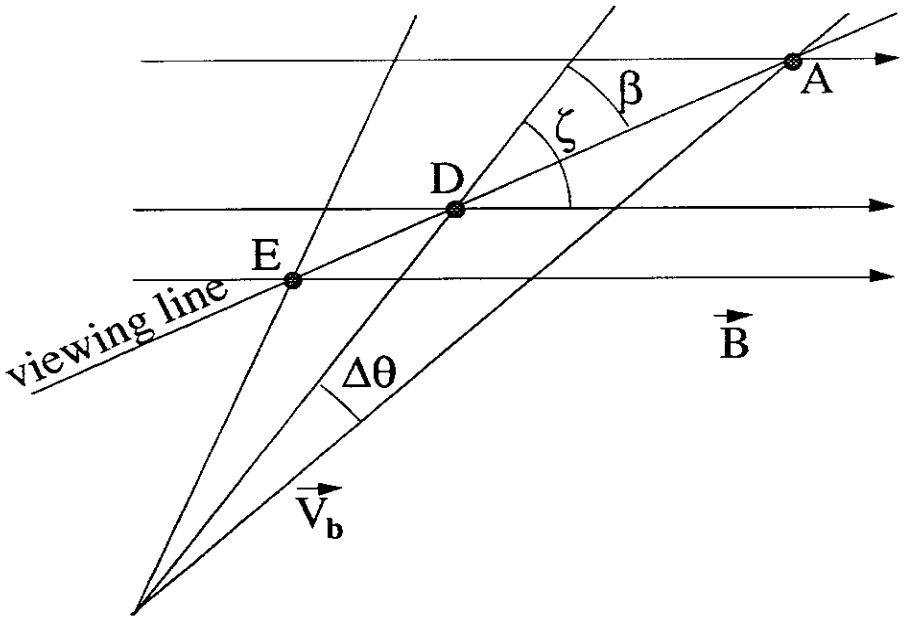

Fig.1

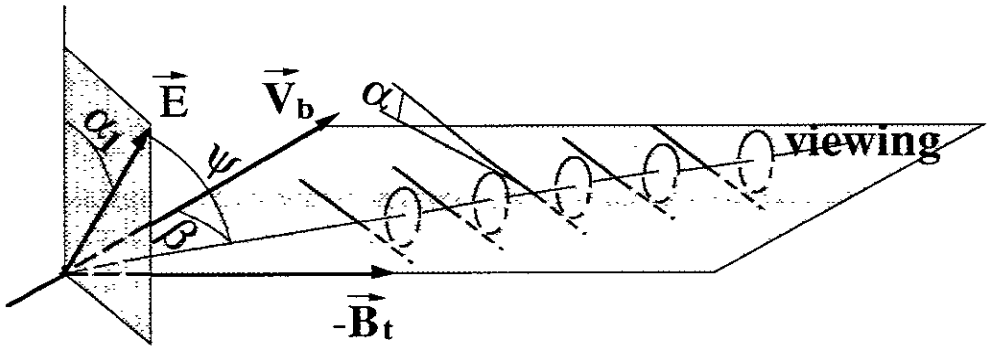

Fig. 2

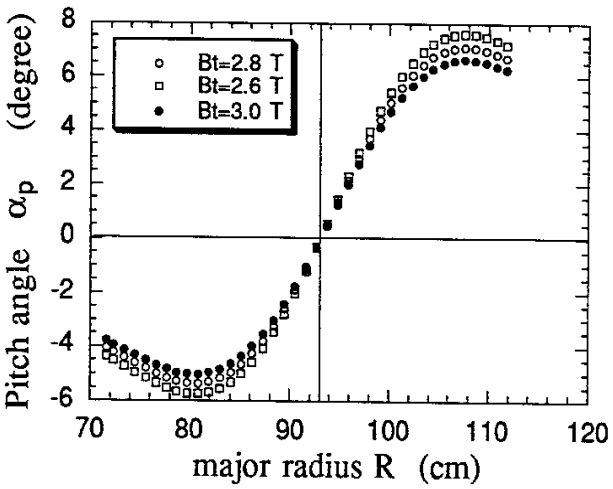
Bt=2.8 T
Bt=2.6 T
Bt=3.0 T
Pitch angle α_p (degree)
major radius R (cm)

Fig. 3

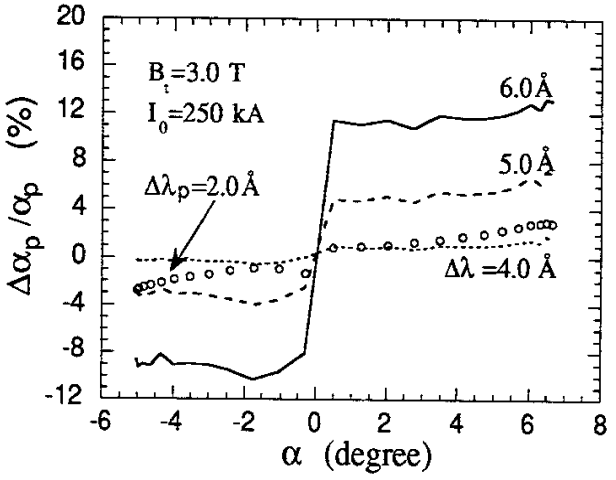
B_t=3.0 T
I_0=250 kA
$\Delta\lambda_p$=2.0 Å
6.0 Å
5.0 Å
$\Delta\lambda$ =4.0 Å
$\Delta\alpha_p/\alpha_p$ (%)
α (degree)

Fig.4

Recent Issues of NIFS Series

NIFS-303 S. Okamura, K. Matsuoka, K. Nishimura, K. Tsumori, R. Akiyama, S. Sakakibara, H. Yamada, S. Morita, T. Morisaki, N. Nakajima, K. Tanaka, J. Xu, K. Ida, H. Iguchi, A. Lazaros, T. Ozaki, H. Arimoto, A. Ejiri, M. Fujiwara, H. Idei, A. Iiyoshi, O, Kaneko, K. Kawahata, T. Kawamoto, S. Kubo, T. Kuroda, O. Motojima, V.D. Pustovitov, A. Sagara, C. Takahashi, K. Toi and I. Yamada,
High Beta Experiments in CHS; Sep. 1994 (IAEA-CN-60/A-2-IV-3)

NIFS-304 K. Ida, H. Idei, H. Sanuki, K. Itoh, J. Xu, S. Hidekuma, K. Kondo, A. Sahara, H. Zushi, S.-I. Itoh, A. Fukuyama, K. Adati, R. Akiyama, S. Bessho, A. Ejiri, A. Fujisawa, M. Fujiwara, Y. Hamada, S. Hirokura, H. Iguchi, O. Kaneko, K. Kawahata, Y. Kawasumi, M. Kojima, S. Kubo, H. Kuramoto, A. Lazaros, R. Liang, K. Matsuoka, T. Minami, T. Mizuuchi, T. Morisaki, S. Morita, K. Nagasaki, K. Narihara, K. Nishimura, A. Nishizawa, T. Obiki, H. Okada, S. Okamura, T. Ozaki, S. Sakakibara, H. Sakakita, A. Sagara, F. Sano, M. Sasao, K. Sato, K.N. Sato, T. Saeki, S. Sudo, C. Takahashi, K. Tanaka, K. Tsumori, H.Yamada, I. Yamada, Y. Takita, T. Tuzuki, K. Toi and T. Watari,
Control of Radial Electric Field in Torus Plasma; Sep. 1994
(IAEA-CN-60/A-2-IV-2)

NIFS-305 T. Hayashi, T. Sato, N. Nakajima, K. Ichiguchi, P. Merkel, J. Nührenberg, U. Schwenn, H. Gardner, A. Bhattacharjee and C.C.Hegna,
Behavior of Magnetic Islands in 3D MHD Equilibria of Helical Devices;
Sep. 1994 (IAEA-CN-60/D-2-II-4)

NIFS-306 S. Murakami, M. Okamoto, N. Nakajima, K.Y. Watanabe, T. Watari, T. Mutoh, R. Kumazawa and T. Seki,
Monte Carlo Simulation for ICRF Heating in Heliotron/Torsatrons;
Sep. 1994 (IAEA-CN-60/D-P-I-14)

NIFS-307 Y. Takeiri, A. Ando, O. Kaneko, Y. Oka, K. Tsumori, R. Akiyama, E. Asano, T. Kawamoto, T. Kuroda, M. Tanaka and H. Kawakami,
Development of an Intense Negative Hydrogen Ion Source with a Wide-Range of External Magnetic Filter Field; Sep. 1994

NIFS-308 T. Hayashi, T. Sato, H.J. Gardner and J.D. Meiss,
Evolution of Magnetic Islands in a Heliac; Sep. 1994

NIFS-309 H. Amo, T. Sato and A. Kageyama,
Intermittent Energy Bursts and Recurrent Topological Change of a Twisting Magnetic Flux Tube; Sep.1994

NIFS-310 T. Yamagishi and H. Sanuki,
Effect of Anomalous Plasma Transport on Radial Electric Field in Torsatron/Heliotron; Sep. 1994

NIFS-311 K. Watanabe, T. Sato and Y. Nakayama,
Current-profile Flattening and Hot Core Shift due to the Nonlinear Development of Resistive Kink Mode; Oct. 1994

NIFS-312 M. Salimullah, B. Dasgupta, K. Watanabe and T. Sato,
Modification and Damping of Alfvén Waves in a Magnetized Dusty Plasma; Oct. 1994

NIFS-313 K. Ida, Y. Miura, S -I. Itoh, J.V. Hofmann, A. Fukuyama, S. Hidekuma, H. Sanuki, H. Idei, H. Yamada, H. Iguchi, K. Itoh,
Physical Mechanism Determining the Radial Electric Field and its Radial Structure in a Toroidal Plasma; Oct. 1994

NIFS-314 Shao-ping Zhu, R. Horiuchi, T. Sato and The Complexity Simulation Group,
Non-Taylor Magnetohydrodynamic Self-Organization; Oct. 1994

NIFS-315 M. Tanaka,
Collisionless Magnetic Reconnection Associated with Coalescence of Flux Bundles; Nov. 1994

NIFS-316 M. Tanaka,
Macro-EM Particle Simulation Method and A Study of Collisionless Magnetic Reconnection; Nov. 1994

NIFS-317 A. Fujisawa, H. Iguchi, M. Sasao and Y. Hamada,
Second Order Focusing Property of 210° Cylindrical Energy Analyzer; Nov. 1994

NIFS-318 T. Sato and Complexity Simulation Group,
Complexity in Plasma - A Grand View of Self- Organization; Nov. 1994

NIFS-319 Y. Todo, T. Sato, K. Watanabe, T.H. Watanabe and R. Horiuchi,
MHD-Vlasov Simulation of the Toroidal Alfvén Eigenmode; Nov. 1994

NIFS-320 A. Kageyama, T. Sato and The Complexity Simulation Group,
Computer Simulation of a Magnetohydrodynamic Dynamo II: Nov. 1994

NIFS-321 A. Bhattacharjee, T. Hayashi, C.C.Hegna, N. Nakajima and T. Sato,
Theory of Pressure-induced Islands and Self-healing in Three-dimensional Toroidal Magnetohydrodynamic Equilibria; Nov. 1994

NIFS-322 A. Iiyoshi, K. Yamazaki and the LHD Group,
Recent Studies of the Large Helical Device; Nov. 1994

NIFS-323 A. Iiyoshi and K. Yamazaki,
The Next Large Helical Devices; Nov. 1994

NIFS-324 V.D. Pustovitov
Quasisymmetry Equations for Conventional Stellarators; Nov. 1994

NIFS-325 A. Taniike, M. Sasao, Y. Hamada, J. Fujita, M. Wada,
The Energy Broadening Resulting from Electron Stripping Process of a Low Energy Au^- Beam; Dec. 1994

NIFS-326 I. Viniar and S. Sudo,
New Pellet Production and Acceleration Technologies for High Speed Pellet Injection System "HIPEL" in Large Helical Device; Dec. 1994

NIFS-327 Y. Hamada, A. Nishizawa, Y. Kawasumi, K. Kawahata, K. Itoh, A. Ejiri, K. Toi, K. Narihara, K. Sato, T. Seki, H. Iguchi, A. Fujisawa, K. Adachi, S. Hidekuma, S. Hirokura, K. Ida, M. Kojima, J. Koong, R. Kumazawa, H. Kuramoto, R. Liang, T. Minami, H. Sakakita, M. Sasao, K.N. Sato, T. Tsuzuki, J. Xu, I. Yamada, T. Watari,
Fast Potential Change in Sawteeth in JIPP T-IIU Tokamak Plasmas; Dec. 1994

NIFS-328 V.D. Pustovitov,
Effect of Satellite Helical Harmonics on the Stellarator Configuration; Dec. 1994

NIFS-329 K. Itoh, S-I. Itoh and A. Fukuyama,
A Model of Sawtooth Based on the Transport Catastrophe; Dec. 1994

NIFS-330 K. Nagasaki, A. Ejiri,
Launching Conditions for Electron Cyclotron Heating in a Sheared Magnetic Field; Jan. 1995

NIFS-331 T.H. Watanabe, Y. Todo, R. Horiuchi, K. Watanabe, T. Sato,
An Advanced Electrostatic Particle Simulation Algorithm for Implicit Time Integration; Jan. 1995

NIFS-332 N. Bekki and T. Karakisawa,
Bifurcations from Periodic Solution in a Simplified Model of Two-dimensional Magnetoconvection; Jan. 1995

NIFS-333 K. Itoh, S.-I. Itoh, M. Yagi, A. Fukuyama,
Theory of Anomalous Transport in Reverse Field Pinch; Jan. 1995

NIFS-334 K. Nagasaki, A. Isayama and A. Ejiri
Application of Grating Polarizer to 106.4GHz ECH System on Heliotron-E; Jan. 1995

NIFS-335 H. Takamaru, T. Sato, R. Horiuchi, K. Watanabe and Complexity Simulation Group,
A Self-Consistent Open Boundary Model for Particle Simulation in Plasmas; Feb. 1995

NIFS-336 B.B. Kadomtsev,

Quantum Telegragh : is it possible?; Feb. 1995

NIFS-337 B.B.Kadomtsev,
Ball Lightning as Self-Organization Phenomenon; Feb. 1995

NIFS-338 Y. Takeiri, A. Ando, O. Kaneko, Y. Oka, K. Tsumori, R. Akiyama, E. Asano, T. Kawamoto, M. Tanaka and T. Kuroda,
High-Energy Acceleration of an Intense Negative Ion Beam; Feb. 1995

NIFS-339 K. Toi, T. Morisaki, S. Sakakibara, S. Ohdachi, T.Minami, S. Morita, H. Yamada, K. Tanaka, K. Ida, S. Okamura, A. Ejiri, H. Iguchi, K. Nishimura, K. Matsuoka, A. Ando, J. Xu, I. Yamada, K. Narihara, R. Akiyama, H. Idei, S. Kubo, T. Ozaki, C. Takahashi, K. Tsumori,
H-Mode Study in CHS; Feb. 1995

NIFS-340 T. Okada and H. Tazawa,
Filamentation Instability in a Light Ion Beam-plasma System with External Magnetic Field; Feb. 1995

NIFS-341 T. Watanbe, G. Gnudi,
A New Algorithm for Differential-Algebraic Equations Based on HIDM; Feb. 13, 1995

NIFS-342 Y. Nejoh,
New Stationary Solutions of the Nonlinear Drift Wave Equation; Feb. 1995

NIFS-343 A. Ejiri, S. Sakakibara and K. Kawahata,
Signal Based Mixing Analysis for the Magnetohydrodynamic Mode Reconstruction from Homodyne Microwave Reflectometry; Mar.. 1995

NIFS-344 B.B.Kadomtsev, K. Itoh, S.-I. Itoh
Fast Change in Core Transport after L-H Transition; Mar. 1995

NIFS-345 W.X. Wang, M. Okamoto, N. Nakajima and S. Murakami,
An Accurate Nonlinear Monte Carlo Collision Operator; Mar. 1995

NIFS-346 S. Sasaki, S. Takamura, S. Masuzaki, S. Watanabe, T. Kato, K. Kadota,
Helium I Line Intensity Ratios in a Plasma for the Diagnostics of Fusion Edge Plasmas; Mar. 1995

NIFS-347 M. Osakabe,
Measurement of Neutron Energy on D-T Fusion Plasma Experiments; Apr. 1995

NIFS-348 M. Sita Janaki, M.R. Gupta and Brahmananda Dasgupta,
Adiabatic Electron Acceleration in a Cnoidal Wave; Apr. 1995